Brine Exclusion Process from Growing Sea Ice*

by

Masaaki WAKATSUCHI
若 土 正 曉
The Institute of Low Temperature Science

Received December 1983

Abstract

The exclusion process of brine from growing sea ice, which plays an important role in the polar ocean, has been quantitatively studied in the field and laboratory in which sea ice grew under various conditions. From oceanographic observations during the growth of sea ice in the Antarctic winter it was found that a haline convection induced by brine exclusion changed the salinity structure of shelf water from stratified to homogenized distribution, yielding the salinization of the water. The appearance of the excluded brine falling into the seawater was experimentally observed by means of a schlieren optical system, with the following findings : The excluded brine formed long vertical filaments starting at fixed positions on the water-ice interface and fell into the underlying seawater without appreciable diffusion. The characteristics of the brine filaments varied with the ice growth rate. At a higher ice growth rate, a larger number of thinner brine filaments fell at a lower velocity. Direct measurements were made of the salinity and volume of the excluded brine under various conditions of ice growth. The brine salinity increases and the volume flux decreases as the ice growth rate decreases. Consequently, the salt flux of the brine decreases with decreasing ice growth rate and hence the amount of salt excluded as brine depends highly upon its volume rather than its salinity. For sea ice growth rates between 1.7×10^{-5} and 1.4×10^{-4} cm・s^{-1}, and for a seawater salinity of 33.0‰, the brine salinity ranged from 42.3 to 92.7‰, the volume flux ranged from 6.3×10^{-6} to 3.4×10^{-5} cc・cm^{-2}・s^{-1}, and the salt flux ranged from 6.4×10^{-7} to 1.5×10^{-6} g・cm^{-2}・s^{-1}. The total volume of brine excluded during one sequence of ice formation depends upon the duration of formation as well as the ice growth rate. It increases with an increase in both growth rate and duration ; that is, with an increase in the mass of ice grown. The brine exclusion process thus disclosed sheds light on a change in salinity of natural sea ice under various conditions of ice growth. When it takes a longer time for a sea ice to grow to a fixed thickness, the sea ice has a lower salinity. This is due to the exclusion of a larger amount of brine with a higher salinity during the formation of sea ice. Meanwhile, a thicker sea ice grown during a fixed period of time has a higher salinity. This is due to the exclusion of a smaller amount of brine with a lower salinity per unit mass of ice grown during the period. The foregoing results suggest that the salinity and volume of brine excluded during the formation of sea ice can be estimated approximately in future by measuring the duration of formation, thickness and salinity of the sea ice.

* Contribution No. 2627 from the Institute of Low Temperature Science
北海道大学審査学位論文

Contents

I. Introduction

In the polar ocean, Arctic and Antarctic, atmospheric cooling freezes the water surface and forms sea ice on it. The rate of sea ice growth, which changes with such cooling conditions as air temperature, wind speed and radiation, determines the structure of the sea ice thus formed.

It is well known that growing sea ice excludes brine which is at low temperature and has high salinity and hence the formed sea ice has salinity less than that of the original seawater. The sea ice salinity also depends upon the ice growth rate. Since the excluded brine is denser than the underlying seawater, the brine exclusion induces a haline convection [Foster, 1969, 1972 ; Farhadieh and Tankin, 1972 ; Wakatsuchi, 1977].With progress in ice growth the haline convection is further invigorated, yielding an appreciable salinization of shallow shelf water in the Antarctic winter [Brennecke, 1921 ; Wakatsuchi, 1982]. Gill [1973] points out theoretically that the salinity increased shelf water sinks along the slope of the continental shelf mixing with deeper water, and that Antarctic Bottom Water may be formed through the convective-mixing process. Though the formation process of Antarctic Bottom Water is not yet completely understood, it is now widely believed from the works of Brennecke [1921] and Mosby [1934] that the primary influence upon the formation process is the exclusion of brine from growing sea ice.

The present study aims at a quantitative understanding of the brine exclusion process, which has a marked influence upon various phenomena in the polar ocean, as mentioned above. In this connection, the next section II is devoted to the results of observations concerning the salinization, with progress in ice growth, of shallow shelf water in the Antarctic region during the winter. Then, explained in section III are sea ice characteristics, structure and salinity, as a function of ice growth rate. The amount of salt excluded during the ice formation has been estimated through the measurements of salinities of the formed sea ice and the original seawater. Little has been understood, however, about the process of salt exclusion. The observation results about how the excluded brine falls into the underlying seawater, which were obtained with a schlieren optical system, are described in section IV. Finally the results of direct measurements of the salinity and volume of the excluded brine under various ice growing conditions are presented in section V.

II. Salinization of shallow shelf water during ice growth process

Oceanographic observations under the growing sea ice sheet were carried out near Syowa Station (69°S and 39.5°E) in Lützow-Holm Bay, Antarctica, from March 1976 to January 1977, to examine how the salinity of shallow shelf water increases as a result of brine

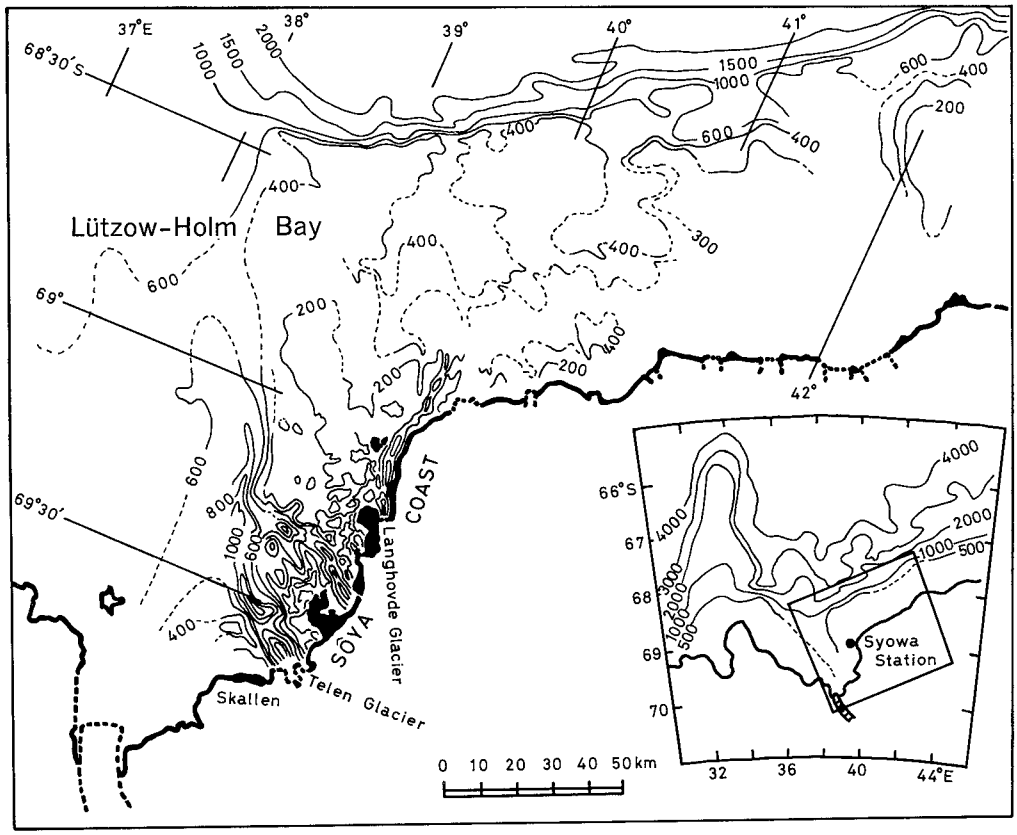

Fig. 1 Bathymetry of Lützow-Holm Bay.

exclusion accompanied with growth of sea ice. Figure 1 shows a bathymetry in Lützow-Holm Bay. This station is located on Ongul Island in the bay. The continental shelf spreads here with the mean width of 60 km and the mean depth of 300-400 m. Several glacial troughs and narrow channels deeper than 600 m are found near the Sôya Coast [Fujiwara, 1971]. Since the sea surface in this area was already covered with fast ice sheets thicker than 1 m, oceanographic observations during the initial process of freezing were performed in an artificially made pool ; it was a square hole made by removing ice blocks of 5 m×5 m in area from the ice sheet. The opened seawater surface in the pool was exposed to cold air and sea ice newly grew there. In addition to the above observations, seasonal variations in water structure under the fast ice sheet were observed at several stations located over glacial troughs and narrow channels near the Sôya Coast.

II. 1. *Pool experiment*

The pool was located over a small basin (about 55 m deep) within an extremely shallow

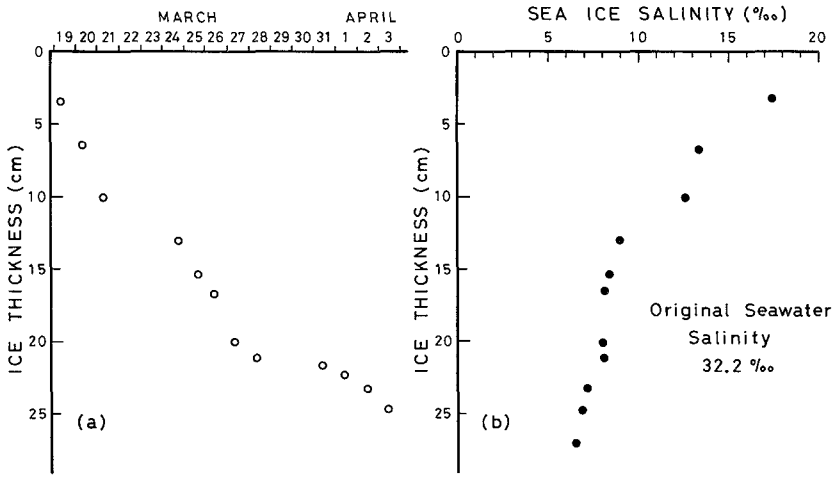

Fig. 2 Ice thickness vs. date of measurement (a) ; Bulk ice salinity vs. thickness (b).

continental shelf with a mean depth of about 30−40 m just near Syowa Station. Sea ice grew to about 25 cm thick in the pool during the observation period from March 18 to April 3 in 1976 and its bulk salinity decreased with an increase in thickness of growing sea ice, as shown in Figure 2. The water salinity profiles under the sea ice were continuously obtained by lowering a portable salinometer (Type MC5/2, made in England).

With an increase in thickness of ice and a decrease in its salinity, the salinity of the underlying seawater increased appreciably, as shown in Figure 3. Although the seawater temperature profiles were also obtained at the same time, they changed little during the observation period and the temperature of the entire water column was near the equilibrium freezing point. Because of the strong salinity dependence of density at low temperature, salinity profiles, which are shown in Figure 3, can also be regarded as density profiles. To follow simply the sequence of salinization of seawater, the salinity profiles were extracted from Figure 3 at three typical

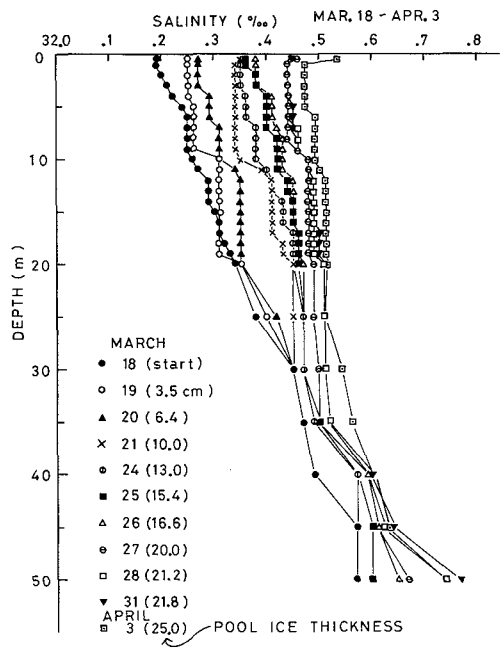

Fig. 3 Change in water-salinity profiles under growing sea ice in the pool.

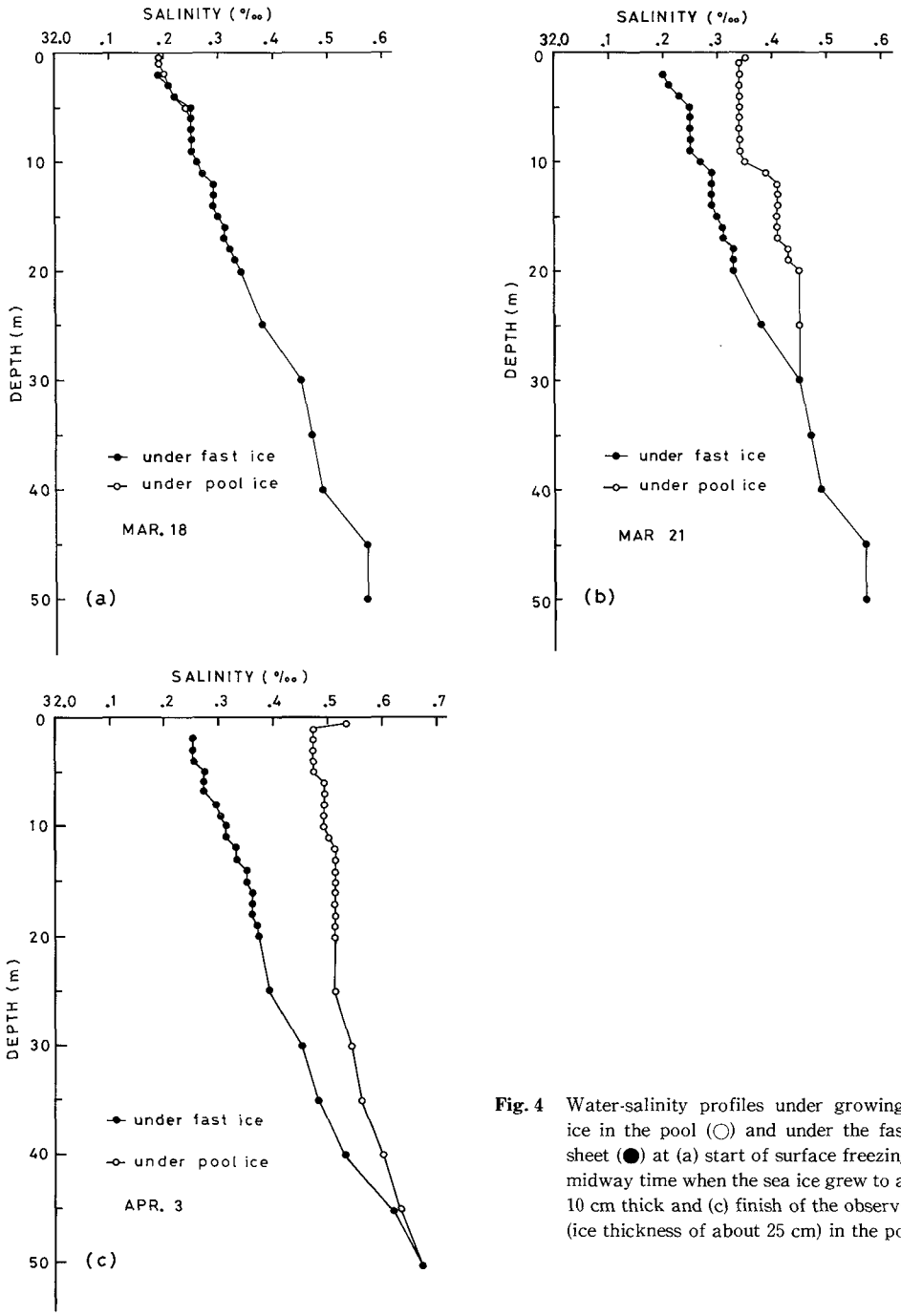

Fig. 4 Water-salinity profiles under growing sea ice in the pool (○) and under the fast ice sheet (●) at (a) start of surface freezing, (b) midway time when the sea ice grew to about 10 cm thick and (c) finish of the observation (ice thickness of about 25 cm) in the pool.

times : the start of surface freezing, a midway point in ice growth and the finish of the observation. They are indicated in Figure 4. It was observed that the salinity structure of the water column in the pool changed from stratified to homogenized distribution and that the depth of layers increasing in salinity lowered.

This sea area was observed to have no current and tidal change between the depths 30 and 80 cm during the observation period. Even in case the tide is considered to cause a change in the salinity profile in the pool, the major change in it should be due to convective mixing induced by the exclusion of brine from the sea ice which has been formed there.

For reference, the salinity profiles were also observed in a water column under the fast ice sheet located about 10 m apart from the pool. The observation results are plotted in Figure 4 against the data in the pool obtained simultaneously. Since the mature fast ice (about 2 m thick) grew only by about 2 cm in thickness during the observation period, the salinization of the underlying seawater was found little, as expected.

II. 2. *Oceanographic observations*

Oceanographic observations were carried out at least once a month from May to December in 1976, using standard Nansen bottles and paired reversing thermometers in a low temperature range (−2 to 10°C). The sea surface at the start of observation had already been covered with an old ice as thick as 80 cm and the ice grew to the thickness of about 2 m by the end of the winter. An ice hole of about 30 cm in diameter was bored with an electric core drill and the obtained ice cores were saved for measuring ice salinity profiles. Water temperature and salinity profiles were measured through the ice hole. The observation results obtained in the Ongul Strait are shown as an example in Figures 5 and 6.

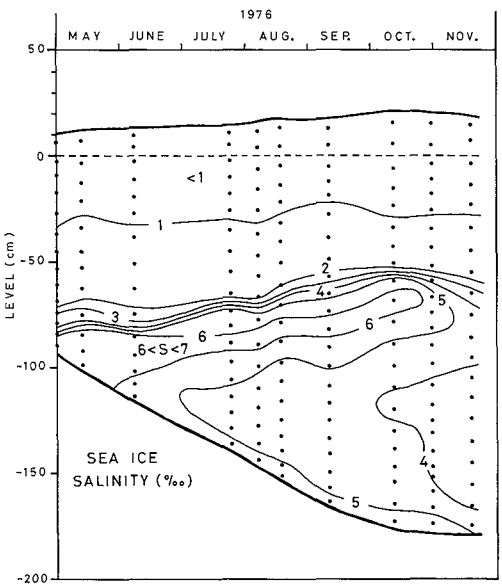

Fig. 5 Seasonal variations in sea-ice salinity profiles in the Ongul Strait. The broken line represents the sea level, and the dots indicate locations of ice samples collected.

Since the old ice kept relatively low salinities (less than 2‰) throughout the observation period, a distinct boundary is shown between the parts of old ice and newly accreted ice in the salinity profiles, as shown in Figure 5. In the latter a relatively high salinity layer produced initially was kept in the original level changing little in salinity, whereas salinities in the underlying layers gradually decreased during the growth process.

Since the sea ice originates from seawater with a salinity of about 33.5‰, the salinity decrease would lead to a salinization in the underlying water column, if no lateral advection exists there.

In May when the observation started, the seawater column of the Ongul Strait was found to have had a stratified structure concerning salinity already, as shown in Figure 6. In this figure surface water less than 33.5‰ in salinity seems to be a remnant of the layer diluted by ice melting in summer. The figure provides the following interpretation ; from May to July the salinity of the water column above a depth of 200 m gradually increased and the water temperature lowered with progress in ice growth. The stratified structure composed of superimposed multi-layers disappeared on July 11 and two homogeneous water masses with the salinities of 33.65 and 33.93‰ were observed over and under a relatively strong halocline at a depth of 50 m. In particular the latter extended from 50 to 300 m in depth. The salinities of both homogeneous water masses increased further during the period from late July to early September when the ice growth rate was relatively high, as shown in Figure 5.

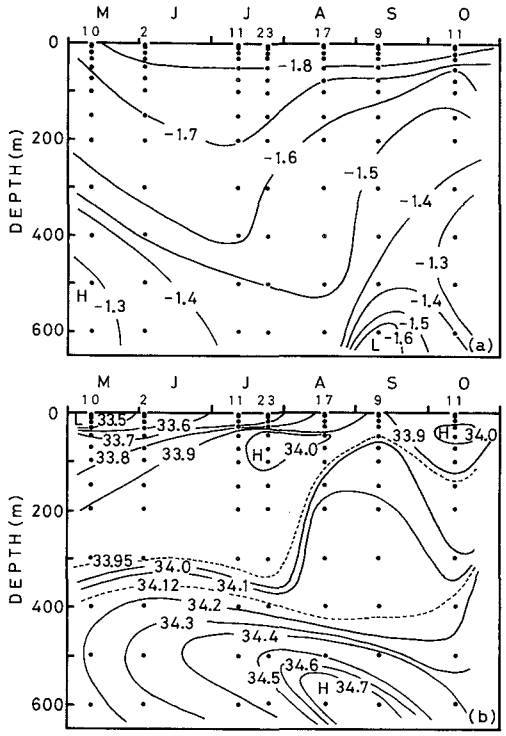

Fig. 6 Seasonal variations in (a) water temperature (℃) and (b) salinity (‰) profiles in the Ongul strait.

Since the upper water mass increased its salinity at a relatively high rate, the seasonal halocline disappeared in early August and one homogeneous water mass was newly observed on September 9. This homogeneous water mass which ranged between 33.9 and 34.12‰ in salinity reached a depth of 400 m, as shown in Figure 6b.

The salinity of the surface water above 400 m increased from 33.87‰ in May to 34.05‰ in September when the ice growth was virtually over with the end of the winter. Meanwhile, the salinity of bottom water under this depth also increased during the ice growth, its maximum attaining to 34.83‰ in mid-August.

In the Ongul Strait, when a stainless cable with Nansen bottles was lowered to the deepest level (600 m), the cable was at a standstill without any inclination. Current measurements were made within the upper layer over the depth of 50 m during the ice growth but no current was observed throughout the observation period. Therefore, the results of the above observation support that the primary cause of the formation of the homogeneous water

above the depth of 400 m is the exclusion of brine from growing sea ice ; that the brine exclusion induces a haline convection ; and that the homogeneous water is produced mainly through the convection process, increasing the salinity of the upper water mass. It follows then that the maximum thickness of the convection layer should be about 400 m in early September. As for the bottom water it remains unknown as yet whether the salinity increase is caused by the brine excluded from the ice which penetrated through the convection layer and reached the bottom layer or by the advection of the surrounding saline water.

II. 3. *Cabbeling effect*

It is considered from both the results of observations in the pool and the Ongul Strait that the major cause in salinization of shallow shelf water is the haline convection induced by the exclusion of brine from growing sea ice. The following is a qualitative proposal for a possible mechanism of salinization using a *T-S* diagram indicated in Figure 7.

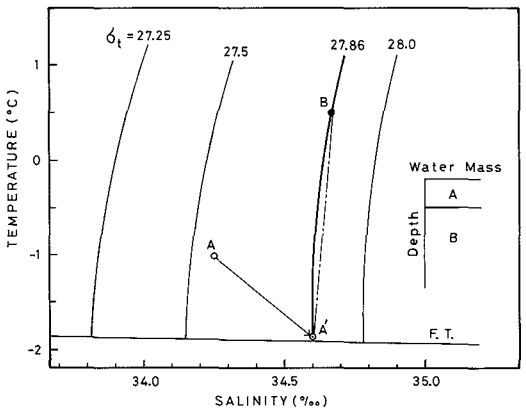

Fig. 7 Temperature-salinity diagram. F. T., equilibrium line of freezing temperature. Details in the text.

On the basis of Brennecke's observation data [1921], the surface waters in Weddell Sea at the beginning of winter are characterized by a relatively cold, low salinity surface water (referred to as A) overlying a warmer, more saline water (B). Suppose that the surface water A changes in quality to a water (A′) with the same density as that of the underlying water B by lowering its temperature and increasing its salinity on account of the brine exclusion with progress in ice growth. If A′ mixes partially with B, then the mixed water should become denser than B regardless of the mixing ratio, and it should sink through B into the deeper layer. Therefore, the depth of the convective mixing layer gradually descends through the above process and the entire shelf water column increases the salinity.

III. Sea ice characteristics

III. 1. *Structure of sea ice*

To understand the brine exclusion process, we first must study the internal structure of sea ice. Figure 8 shows schematically the structure of sea ice. According to the previous studies [Tabata and Ono, 1957 ; Weeks, 1958], a normal sea-ice sheet consists of long, vertical

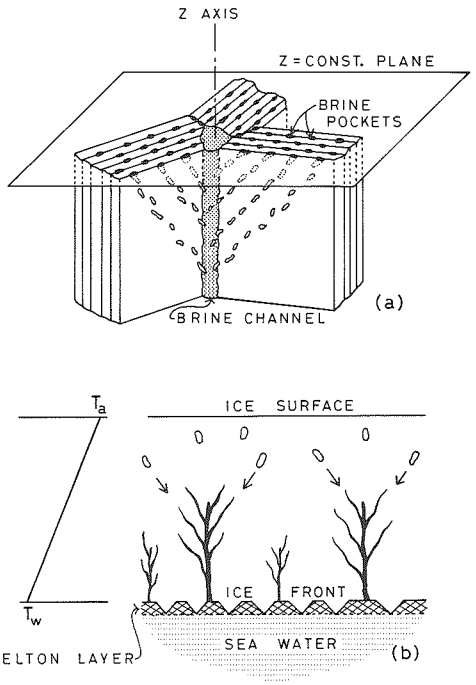

Fig. 8 Schematic diagrams of sea-ice structure. (a) Microscopic drawing of ice crystals, brine pockets and a brine drainage channel ; (b) macroscopic vertical section of tree-shaped channels, T_a and T_w representing air and seawater temperatures, respectively, where $T_a < T_w$.

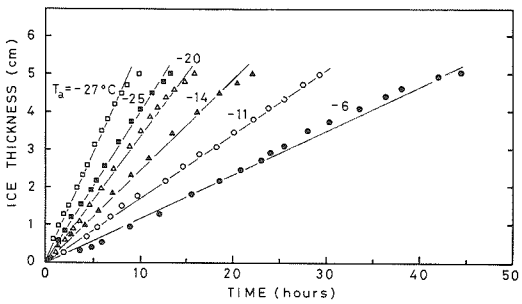

Fig. 9 Change in sea ice growth rate with air temperature (T_a).

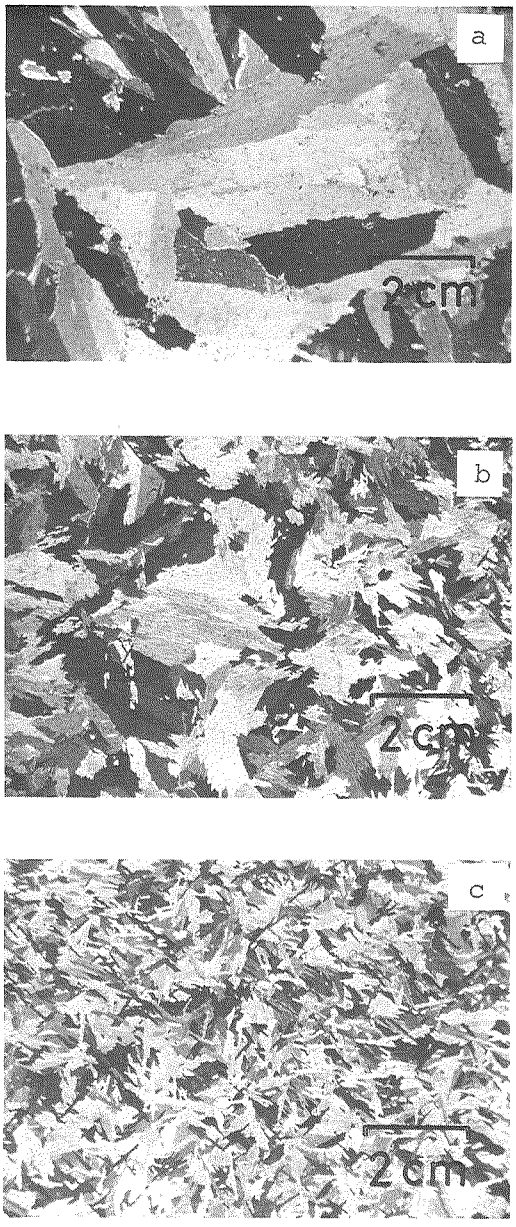

Fig. 10 Horizontal sections of sea ices at the depth of 2.2 cm formed at growth rates : (a) 0.185 cm · h^{-1}, (b) 0.33 cm · h^{-1} and (c) 0.49 cm · h^{-1}.

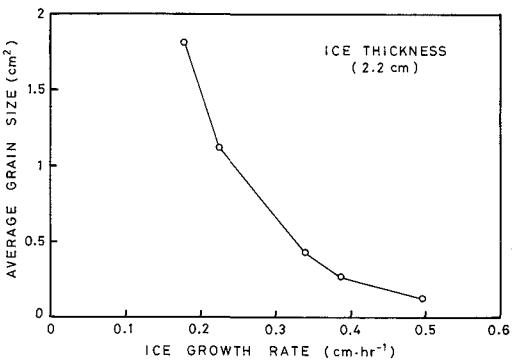

Fig. 11 Average grain size vs. ice growth rate.

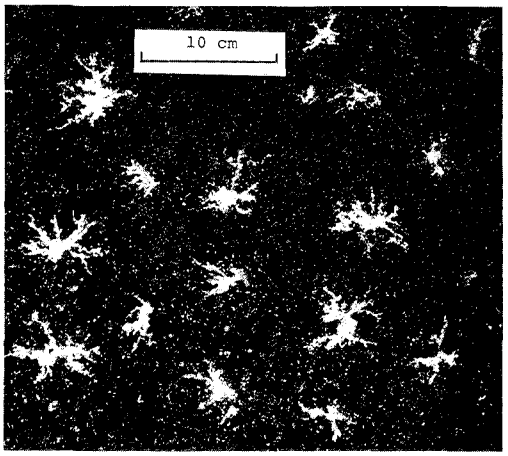

Fig. 12 Horizontal section of brine drainage channels, each resembling the shape of a bright star.

ice crystals, each usually several centimetres square in horizontal cross section, frequently also much smaller. In addition, each ice crystal consists of parallel pure ice plates in the direction of growth and the thicknesses of ice plates are 0.3-0.6 mm. The crystal structure of sea ice changes markedly with ice growth rate.

Sea ice increases its thickness linearly with time during the initial growing process, at least up to 5 cm thick, as shown in Figure 9. The ice growth rate increases with lowering air temperature. With an increase in ice growth rate the grain size becomes smaller (see both Figures 10 and 11).

Brine pockets are contained between the ice plates and between the ice crystals. Brine channels distribute frequently in boundary areas where two or more ice crystals intersect with one another [Saito and Ono, 1980 ; Wakatsuchi et al., 1982]. Generally a brine channel takes the form of a tree, consisting of a large vertical tubular structure attended by smaller tributary tubes, as shown in Figure 8b. The diameters of them change from less than 1 to several mm.

The spatial density of brine channels has been examined by several investigators since Bennington [1963] first found the presence of them. The brine channels of a new ice distribute homogeneously in space, as shown in Figure 12. For a thick sea ice Lake and Lewis [1970] gave excellent examples of brine channels. From field observations they reported on the density of one large brine tube per 180 cm^2 with a diameter larger than 5 mm in an ice sample 1.6 m in thickness, as well as on the density of 42 tubes per cm^2, their being small tubes less than 1 mm in diameter, averaging 0.4 mm. Meanwhile, Martin [1979], using the same set of data, obtained the density of one channel per 100 cm^2. In other field investigations, Bennington [1967] observed one large open channel per 800 cm^2 in a sample 0.2 m in thickness.

Such a wide scattering in spatial density originates from the use of different ice samples in disregard of growth history. Saito and Ono [1980], therefore, examined experimentally the spatial density of brine channels as a function of ice growth rate. According to them, the spatial density increases with increasing ice growth rate, as shown in Figure 13.

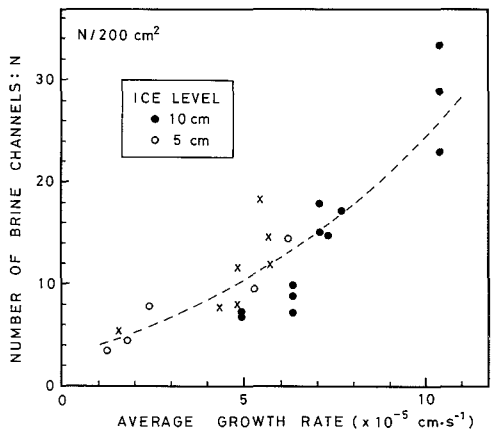

Fig. 13 Spatial density of brine channels vs. ice growth rate (○ ● after Saito and Ono [1980] ; x after Wakatsuchi et al. [1982]).

III. 2. *Desalination of sea ice*

Exposure of the sea ice surface to cold air and the contact of its bottom with warmer seawater give rise to a temperature gradient within the sea ice. As a result, brine pockets, which are scattered within the sea ice, freeze on their colder top side and melt on their warmer bottom to keep the thermodynamic equilibrium ; then, the brine pockets migrate toward the ice bottom. As noted by Untersteiner [1968], however, the rate of brine pocket migration is fairly slow (less than 1 mm per day).

As the sea ice becomes colder, the brine in the pockets freezes to form more ice so that the remaining brine increases in salinity. Because the newly formed ice occupies 10% more volume than the brine, the resultant pressure increase expels the brine through cracks and channels into the seawater.

The freezing front of sea ice sheet is characterized by an irregular surface with numerous disconnected ice platelets protruding downward. The ice-water interface, namely a skelton layer, consists of the ice platelets and the brine rejected with the formation of them. Brine exclusion occurs mostly at the ice-water interface though parts of the brine pockets are rejected from the interior of ice sheet into the underlying seawater through the brine channels. This is clear from the salinities of newly grown ice and old ice in the Ongul Strait, as shown in Figure 5 ; namely, the new ice originates from the seawater with a salinity of about 33.5‰ and the resultant salinity decrease is about 17-19‰ , whereas the old ice originates from the new ice, and the salinity decrease is about 3-5‰ .

III. 3. *Relation between sea ice salinity and ice growth rate*

During the formation of ice, parts of brine are excluded into the underlying seawater, leaving the remnant entrapped in the sea ice. Brine content in sea ice determines the salinity of it ; hence, stated reversely, its salinity provides information on salt flux in accordance with the exclusion of brine.

Mass of salt ($\triangle M_S$) that is excluded through unit ice area during the formation of ice by a thickness of $\triangle I$ is expressed by

$$\triangle M_S = S_o(1 - S_i/S_o)\rho_i \triangle I \quad (1)$$

where ρ_i, S_i and S_o represent the density of a sea ice, its salinity and the salinity of an original seawater, respectively. Given the value of ρ_i, then $\triangle M_S$ should be easily derived by measuring values of S_o, S_i and $\triangle I$. According to Weeks and Lee [1958], the density of the new ice may be regarded as 0.945 g · cm^{-3}. Using this and measured values of S_o, S_i and $\triangle I$, we can estimate the salt flux ($\triangle M_S/\triangle t$, where $\triangle t$ represents time during which ice grew by the thickness of $\triangle I$) as a function of the ice growth rate ($\triangle I/\triangle t$).

Shown in Figure 14 are bulk salinities of sea ice which formed, under various conditions, in the field and laboratory. Common to all samples, the sea ice salinity decreases with an increase in both thickness and duration of formation. Let the rate of ice growth be defined as the amount of ice thickness divided by duration of formation. Then, in Figure 14 it corresponds to the gradient of a straight line passing through the origin of the coordinate axes. The sea ice salinity is given in Figure 15 as a function of the ice growth rate defined above. In this figure, the laboratory data of Cox and Weeks [1975] on an NaCl ice are also plotted. All these data compare reasonably well with one another in spite of large differences in laboratory and natural conditions. As shown in Figure 15, the sea ice salinity increases with an increase in ice growth rate, its minimum and maximum being about 20 and 60% of the original seawater salinity, respectively. The salt flux obtained using Equation (1) increases with increasing ice growth rate, as shown in Figure 16. It is clear from Figures 15 and 16 that with an increase in ice growth rate both the inclusion and the exclusion of salt

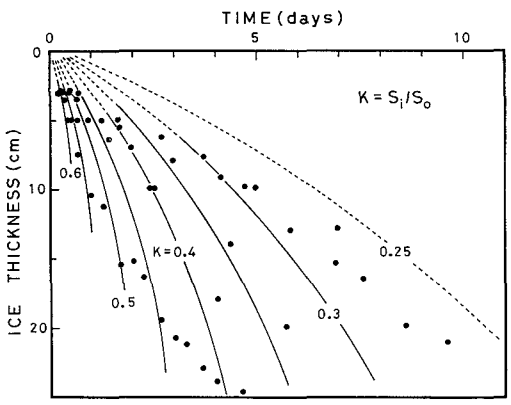

Fig. 14 Changes in K, salinity ratio of sea ice to original seawater, with plots based on measured values of formation time and thickness of the sea ice.

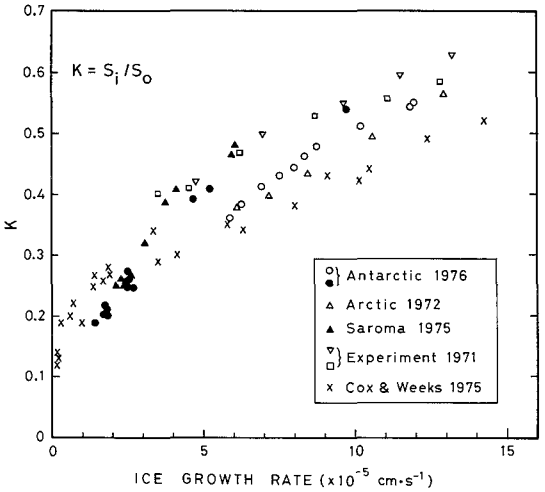

Fig. 15 Salinity ratio (K) vs. ice growth rate.

increase.

As mentioned in this section, ice salinity measurements provide data only on the salt budget during the formation of ice. Data are not available yet on how brine is excluded from growing sea ice into the underlying seawater and how much salinity and volume the excluded brine has.

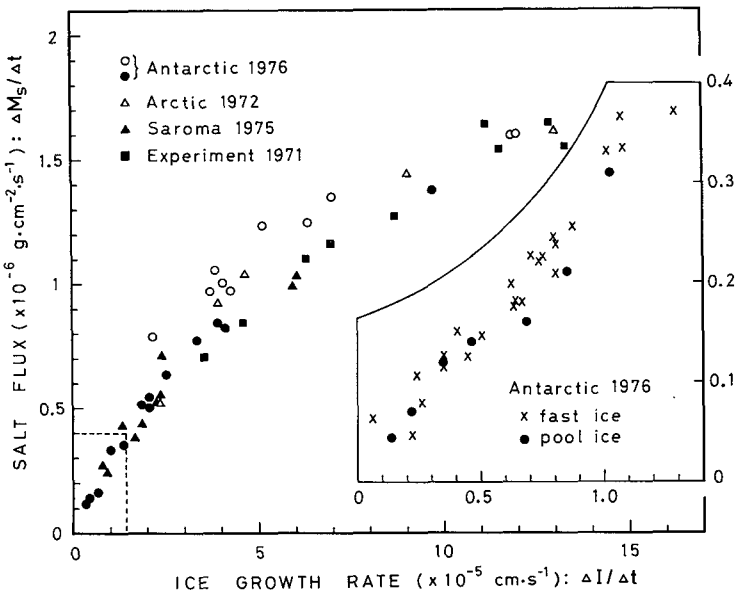

Fig. 16 Salt flux ($\triangle M_s/\triangle t$) vs. ice growth rate ($\triangle I/\triangle t$).

IV. Optical observation of brine streamers

IV. 1. *Experimental apparatus and measurement technique*

The appearance of the excluded brine in seawater was experimentally observed with a schlieren optical system, which is illustrated schematically in Figure 17. Both the parabolic mirrors are 0.45 m in diameter and 4 m in focal distance. They are set face to face approximately 7 m apart. A plate acryl tank with inside dimensions of 20 cm×20 cm×53 cm is placed so that it is closely aligned perpendicular to the light beam. A 16-mm reflex motion picture camera with a time-lapse control system provides the continuous photographic recording of events viewed through the following schlieren optical system : A mercury lamp furnishes a light source and is focused on a slit located at the focal point of the first mirror so that a parallel beam light passes through the tank. A knife edge is located at the focal point of the second mirror and carefully adjusted so that, when there are no dis-

turbances in the tank, the light beam is almost fully cut off. Thus, when the refractive index of a fluid in the tank is locally changed by salinity differences, the light beam is refracted, passes around the knife edge and enters the camera. The entire system is set in a cold room 15 m wide, 5 m long and 3 m high in the clear. Unfortunately, the diameter of the mirrors was too small to make it possible for the camera to cover the whole sight of the tank. To enable it to do so we leveled the camera twice, first at the higher part and then at the lower part of the tank by moving up and down the position of the tank carefully. Although, during the ice growing process, the sides and the bottom of the tank were insulated each with a sheet of styrofoam 0.1 m thick, two of the side sheets perpendicular to the light beam were removed when taking a picture. On account of keeping the tank cooled through the walls, the camera was set in motion only once when the ice thickness reached about 2 cm, and the duration was limited by only about 20 minutes (about 4 frame/s). After having shot an event, we sampled the seawater by inserting an injector with the inside diameter of about 0.5 mm and the length of 15 cm through the side wall. The samples collected from various depths were saved for measuring their salinities. The optical observations were made in two cases of ice growth rates, 8.9×10^{-5} and 14.2×10^{-5} cm · s^{-1}. These rates correspond to the range in which salt rejection is active, as shown in Figure 16.

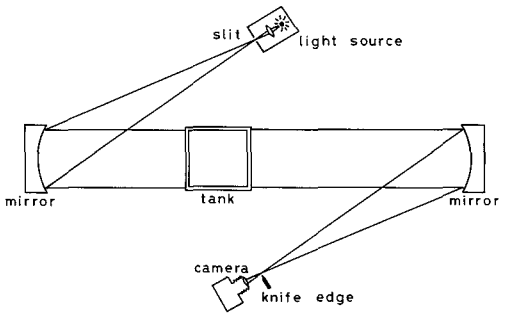

Fig. 17 Schematic diagram of the schlieren optical system.

IV. 2. *Observation results*

The time-lapse motion pictures caught distinctive scenes occurring under growing sea ice. Brine which was rejected, during the formation of ice platelets, at the freezing front of the sea ice remained in the skelton layer for a transient time and then streamed down from definite positions of the layer. The streamers took the form of long vertical filaments and fell into the underlying seawater without appreciable diffusion. The characteristics of the streamers, for instance, diameter, falling velocity and number, varied markedly with the ice growth rate, as shown in Figure 18.

At a higher growth rate, a large number of fine filamentous brines falls in bunches into the underlying seawater. Parts of them turn around about the half way of the tank and ascend upward forming convection cells while diffusing slightly. The maximum horizontal width of a convection cell was about 10 cm. In this case in which convective motion takes place vigorously, the salinity of the seawater column is homogeneous except for the skelton layer which has a high salinity.

Meanwhile, at a lower growth rate, several thicker streamers fall toward the bottom of

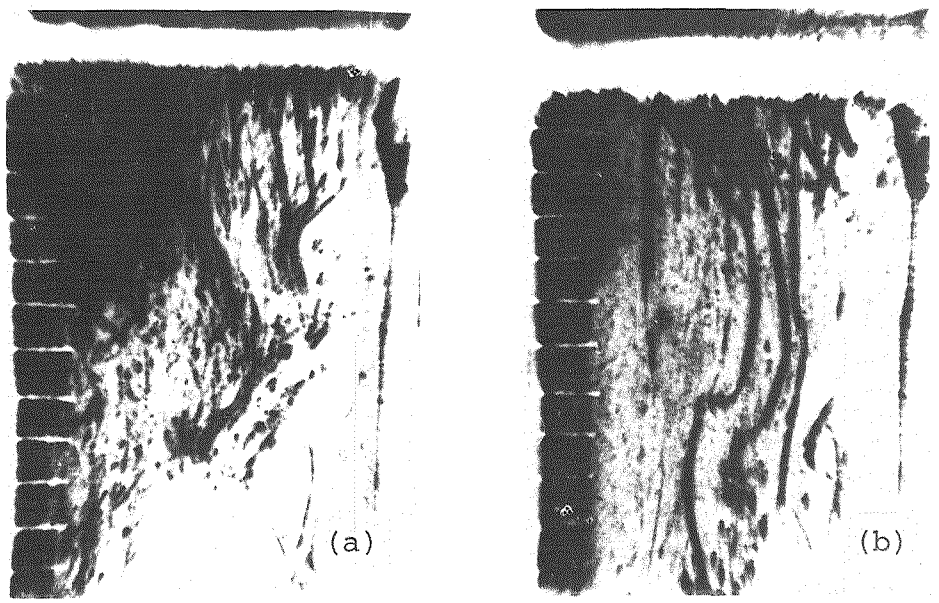

Fig. 18 Schlieren photographs of brine filaments falling from the front of growing sea ice into the underlying seawater at (a) a higher (about 0.51 cm · h^{-1}) and (b) a lower (about 0.32 cm · h^{-1}) growth rate. The upper horizontal bright part is the growing sea ice. A scale of 2-cm interval is indicated on the left.

Table 1 Analytical results of schlieren movie films

No.	Ice Growth Rate ($cm \cdot h^{-1}$)	Salt Flux ($g \cdot cm^{-2} \cdot s^{-1}$)	Brine Filaments				
			Falling Velocity ($cm \cdot s^{-1}$)	Width (cm)	Number	Volume Flux ($cc \cdot cm^{-2} \cdot s^{-1}$)	Salinity (‰)
A	0.51	1.29×10^{-6}	0.21	0.055	30	3.73×10^{-5}	34.58
B	0.32	1.18×10^{-6}	0.39	0.102	4	3.18×10^{-5}	37.11

the tank scarcely with any diffusion. After the streamers strike on the bottom, they spread over there. Hence, part of the surrounding seawater ascends upward in compensation for them. The resultant salinity profile in the seawater column shows a slightly stable structure.

To derive the volume flux of brine we measured the diameter (i. e. the horizontal width) and falling velocity of the individual filaments of the brine and their number with a movie analyzer. The averaged values of them are summarized in Table 1. At the higher growth rate, the volume flux of the individual brine filament is much less since it has the smaller diameter and the slower falling velocity. However, the volume flux of the brine through unit ice area increases slightly at the higher growth rate because of the much larger number of

brine filaments.

Because the salt flux is derived from Equation (1) by measuring the salinities of the original seawater and the formed sea ice, we can approximately estimate the mean salinity of brine filaments by using the salt flux and volume flux. It follows from Table 1 that a thicker brine at a lower growth rate has a higher salinity.

The above observation results, which were obtained with the schlieren optical system, enable us to have an understanding of the effect of the ice growth rate on the salinity and the volume flux of brine, In the next section, we will present a method for finding out the salinity and volume of brine streamers and the measured results.

V. Measurements of salinity and volume of brine streamers falling into seawater

V. 1. *Basic model*

The measurements of the salinity and volume of such brine streamers as seen in Figure 18 are needed to resolve, in future, a problem about how deep they fall down in the seawater with a salinity structure, and to understand the process of convection induced by the exclusion of them. Therefore, we have developed a new technique to trap the brine streamers which fall from a certain area of growing sea ice into the underlying seawater [Wakatsuchi and Ono, 1983].

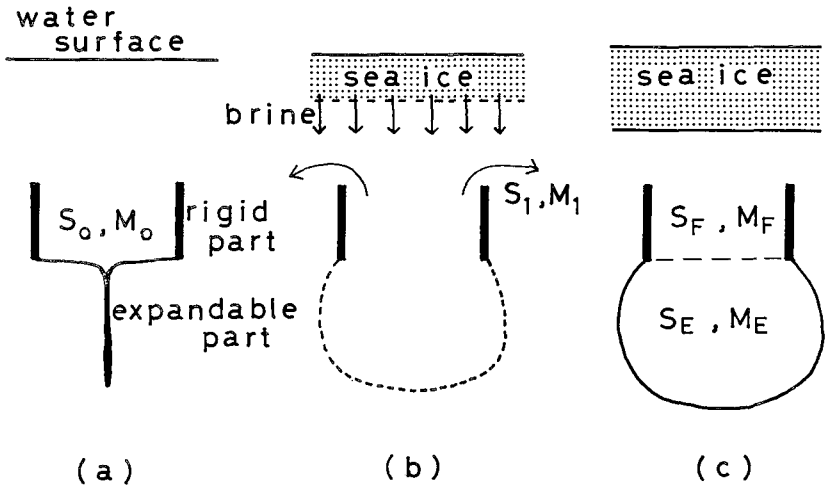

Fig. 19 Modeling on a possible phenomenon which may occur in the sampler while brine is being collected (a) at the start of surface freezing, (b) during the freezing period and (c) at the finish of the collection. Details in the text.

A basic idea as to how such brine streamers which fall into the seawater can be trapped is illustrated in Figure 19. As seen in it, the brine sampler is composed of two part : a rigid container in which they are initially collected and an expandable balloon in which those collected are then trapped, the latter having been previously deflated fully. For accurate measurements of both the salinity and the volume of the brine streamers it is desirable to trap the entire amount of brine streamers in the balloon. However, it is impossible to avoid the overflow of an appreciable amount of brine streamers diluted with seawater, during the trapping of them.

Considering the above technical difficulty, a schematic illustration in Figure 19 may be proposed as a model for phenomena that may occur during the process of the brine collecting. The various notations used in this model are defined as follows ;

(1) The total mass of brine streamers which fall from the bottom of an ice sheet which has the same area as that of the sampler at the top during a freezing period is M_b and the mean salinity of them is S_b. All the excluded brine streamers are assumed to be collected once in the rigid part of the sampler.

(2) The mass and the salinity of an original seawater within the rigid part at the start of surface freezing are M_o and S_o, respectively, and those of salinity-elevated seawater at the finish of brine collection are M_F and S_F, respectively.

(3) The mass and the salinity of the seawater trapped in the expandable part at the finish of brine collection are expressed as M_E and S_E, respectively.

(4) The total mass and the mean salinity of the seawater which overflowed the rigid part during the freezing period are defined as M_1 and S_1, respectively.

According to the above notations, the mass and salt in the brine sampler during the freezing period are budgeted as follows ;

$$M_o + M_b - M_1 = M_F + M_E \tag{2}$$

and

$$S_o M_o + S_b M_b - S_1 M_1 = S_F M_F + S_E M_E \cdot \tag{3}$$

Eliminating M_1 from Equations (2) and (3), we obtain

$$M_b = f_1(S_o,\ M_o,\ S_F,\ M_F,\ S_E,\ M_E,\ S_1 \text{ and } S_b) \tag{4}$$

In the above equation, all the values except for S_1, S_b and M_b can be measured by sampling individual seawaters concerned before and after the experiment. However, there remain three unknown values, S_1, S_b M_b in the above equation, because it was taken into consideration for modeling that the seawater overflowed the rigid part.

Now, let us imagine a freezing process of a seawater under natural conditions. Let us also imagine a water column with the same cross-sectional area as the brine sampler, as shown in Figure 20 ; then, the amount of brine streamers entering the column should be equal

to that entering the sampler. Therefore, the conservation relations for the mass and the salt-mass in the water column can be imaginarily expressed as follows ;

$$M_o = M_i + M_b + M_x \tag{5}$$

and

$$S_o M_o = S_i M_i + S_b M_b + S_o M_x \tag{6}$$

respectively, where M_x represents the mass of the original seawater unconcerned in the freezing process. Using Equations (5) and (6), we obtain

$$M_b = f_2(S_o,\ S_i,\ M_i,\ \textit{and}\ S_b). \tag{7}$$

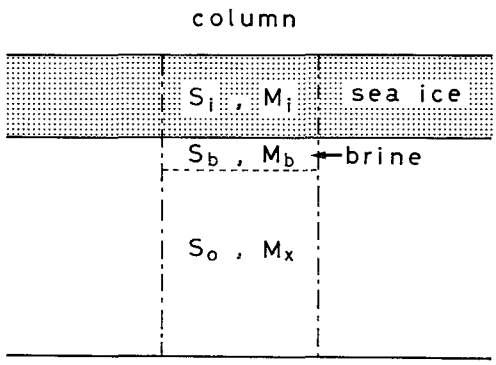

Fig. 20 An imaginary distribution as the result of the freezing of seawater in a water column with the same cross-sectional area as the sampler. Details in the text.

From Equations (4) and (7), the mean salinity of brine streamers is eventually given by

$$S_b = f_3(S_o,\ M_o,\ S_F,\ M_F,\ S_E,\ M_E,\ S_i,\ M_i \text{ and } S_1). \tag{8}$$

If S_1, which is an unmeasurable value, can be approximately given using measurable values, S_b should be derivable by determining the other values in Equation (8). The mean density of brine streamers should be expressed as a function of the mean salinity of them and the corresponding freezing temperature. Substituting the value of S_b thus expected in Equations (4) or (7), therefore, the volume of brine streamers can be determined.

V. 2. *Apparatus and experimental procedures*

The brine sampler used in the present experiment consists of a stainless steel funnel, a small expandable balloon (condom), and a chloroethylene pipe connecting the two, as shown in Figure 21. A steep funnel slope is designed to enable the brine streamers collected by the funnel to remain in the funnel as much as possible . The long and narrow pipe is designed to minimize seawater entrainment. The area of the funnel at the top is about 200 cm^2 (about 16 cm in diameter).

Brine sampling was made in a plastic tank for laboratory work and in artificial pools for field work. As for the tank, it had the shape of a frustum, with the top and the bottom diamerer of about 50 and 44 cm, respectively, and the depth of about 75 cm. The tank was placed in a wooden box for heat insulation and set in a cold room. Meanwhile, as for the field work conducted on the fast ice field (1.5 m thick) off Barrow, Alaska, two artificial pools (2 m×2 m) were prepared by removing ice blocks from the top to the depth of 1 m, leaving the remaining bottom part 0.5 m thick intact, as shown in Figure 22. The underlying seawater was introduced into the pools through a few small holes made in the bottom. The

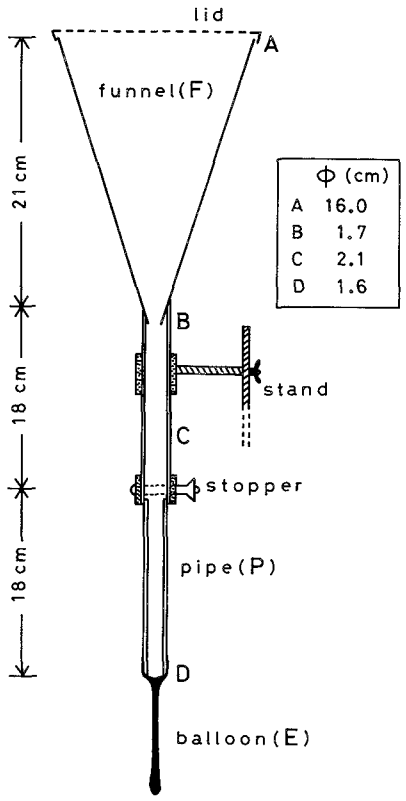

Fig. 21 Illustration of the brine sampler used.

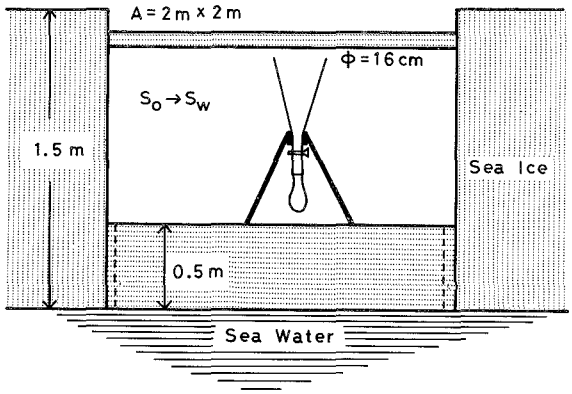

Fig. 22 Schematic diagram of the artificial pool.

holes were virtually closed while an experiment was conducted. One pool had a water depth of 0.85 m and the other 0.9 m.

Upon making the pool, ice was removed off the surfaces of the walls and the bottom of the pool ; then new ice started growing on them as a result of a large heat sink existing in the mass of the surrounding ice sheet. The newly grown ice on them was occasionally removed until ice was no longer growing (about 3 days after the starting of ice removal), and then the experiment was initiated. The two pools were provided to have two ice growth rates by exposing the water surface of the first pool to the atmosphere, while covering that of the second pool entirely with a polyethylene sheet.

Two types of experiments were designed in terms of the conditions of ice. In the first experiment, the ice thickness was limited to range between about 5 and 8 cm in thickness, and the growth rates were changed in a range between 1.7×10^{-5} and 1.4×10^{-4} cm · s^{-1}. Lower rates in this range were covered by the laboratory experiment, and higher rates by the field experiment. Brine streamers were collected continuously until the ice reached the desired thickness. In the second experiment that was performed only in the laboratory, sea ice continued to grow to the thickness of about 15 cm at a constant rate, and brine samplers were changed every 5 cm interval during the growth of ice. The constant growth rate was maintained by lowering the room temperature gradually.

In setting the brine sampler into the tank or the pools, we used the following procedures. After the balloon was fully deflated, the brine sampler was carefully immersed into a seawater. During the immersion, the balloon was held by a hand to prevent the seawater

from flowing into it. When the funnel was filled with seawater to about one-third of the total volume of it, a stopper attached at the middle point of the pipe was closed. Then, the brine sampler was immersed until the stand reached the bottom of the tank or the pools. The initial position of the funnel top was adjusted by changing the height of the stand to keep a space of about 1 cm between the top and the ice front expected at the finishing time of brine collection. The stopper was opened before the surface began freezing. At that time the funnel and the pipe had already been filled with seawater, but the balloon was devoid of it.

At the end of each run of experiment, an ice block of the minimum size was cut out carefully from near the edge of the tank to allow the sampler to be taken out from the tank ; the funnel was immediately covered with a lid and the stopper was closed ; and then the sampler was taken out of the tank or the pools. After another sampler was placed in the tank for the next run of experiment, the ice block was restored to the same position as before ; at this time a small piece of ice was scratched off the block and saved for measurements of salinity.

In the experiment in which the effect of an increase in ice thickness on brine exclusion was examined, the position of the sampler was vertically changed twice in accordance with the position of the ice front during the growth of ice, namely, when ice reached about 5 and 10 cm in thickness, as shown in Figure 23. Since the underlying seawater became higher in

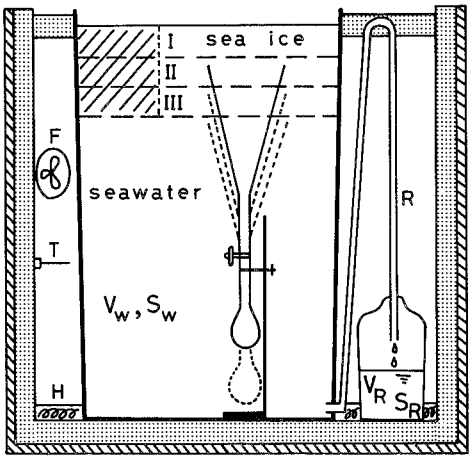

Fig. 23 Illustration of the tank placed in a insulated wooden box. F, fan ; T, thermistor ; H, heater ; R, tube for releasing pressure. The downward change of position of the sampler with ice growth is indicated by the broken lines on the funnel and balloon. The shaded area (left) in ice indicates the place through which we removed the sampler.

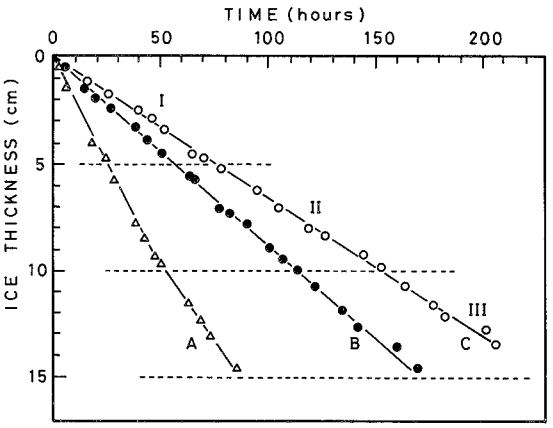

Fig. 24 Ice thickness vs. time of measurement at three constant ice growth rates, 0.170 (A), 0.086 (B) and 0.064 (C) cm · h^{-1}. Stages I, II, III show the first, the second, the third period during which brine was collected.

salinity than the original seawater during the first brine collection, a certain volume of cold fresh water was added with á gentle stirring to bring the salinity near that of the original seawater. The uniformity of salinity was tested at several points in the tank before the subsequent collection of brine.

The ice continued to grow at a nearly constant rate throughout the collection of brine (corresponding to the growth of ice from 0 to 15 cm in thickness), as seen in Figure 24. It took about one hour to change the sampler, during which time ice grew to such a small amount of 0.1 cm in thickness that the amount was excluded from the estimation of growth rate.

Seawater was sampled from three parts of the sampler : the expandable balloon ; the pipe under the stopper ; and the remaining part of the pipe and the funnel. Accordingly, the salinity S and the volume V of each water were suffixed by E, P, and F, respectively, in the above order. Then, measurements were made of S_E, S_P, S_F, V_E, V_P and V_F as well as the salinities of the original seawater, the formed sea ice and the underlying seawater, which were denoted by S_o, S_i and S_w, respectively. Measurements were also made in the laboratory of the volume of the original and the underlying seawater, which were denoted by V_o, and V_w, respectively. In laboratory experiments the pressure generated by ice growth was released through a small tube attached to the bottom of the tank, as shown in Figure 23. The volume V_R and the salinity S_R of the seawater which flowed out through the tube were then subjected to measurements.

V. 3. *Analytical method*

Summarized in Table 2 are the results obtained from all the experimental runs. It is obvious that the seawater trapped in the balloon always displays the highest salinity (S_E), as is expected. Both S_F and S_P exhibit relatively low salinities in comparison with S_E, but they are always found to be higher than S_w, indicating that a significant amount of the brine streamers once collected diffuses within the funnel and the pipe.

The principle of the basic model that was proposed in Section V. 1. is applicable to the case of the present experiment, which keeps the original condition. The analogous model is illustrated schematically in Figure 25. Notations newly used in it are defined as follows :

1. The masses M of brine and seawater are divided by their densities ρ and volumes V.
2. The cross-sectional area of the sampler is expressed as a. The total volume of brine streamers excluded from the bottom of an ice sheet with the same area as the top of the sampler and collected in the funnel during the freezing period ($0<t<T$) is V_{ba}, and the mean density of them as ρ_b.
3. The total volume of the seawater which overflows from the funnel for $0<t<T$ is expessed as V_1, and its mean density as ρ_1.

The total volume defined above should be expressed as

Table 2 Summary of Experimental Results

Experiment Number (No)	Ice Thickness (cm)	Freezing Time (hr)	Mean Air(Room) Temperature (°C)	Seawater Salinity (‰) S_O	S_F	S_P	S_E	S_W	Seawater Volume (cc) V_E
1	6.0	51.0	−10.7	32.95	38.23	42.00	49.43	34.16	159
2	5.5	39.5	−13.2	32.52	36.87	39.85	47.48	33.51	142
3− I	5.5	63.8	− 9.8	33.00	38.88	44.55	55.39	34.42	173
3− II	4.5	50.5	−12.3	33.26	38.68	41.84	57.52	34.68	140
3− III	4.6	56.3	−17.0	33.82	39.91	43.95	58.84	35.50	121
4− I	4.7	69.8	− 5.7	34.09	41.23	47.04	58.30	35.79	189
4− II	4.5	74.8	− 8.0	34.48	42.02	48.27	61.17	36.37	154
4− III	4.0	62.6	−12.1	34.19	41.08	46.16	61.35	36.02	128
5− I	4.8	25.0	−12.0*	33.15	36.40	37.45	43.77	33.84	110
5− II	4.5	23.8	−14.9*	33.47	37.20	38.32	45.54	34.32	95
5− III	5.3	37.3	−19.1*	33.51	38.14	40.05	48.60	34.74	122
6	4.5	18.3	−23.2	32.57	34.63	35.57	41.86	32.90	68
7	5.5	17.8	−23.2	32.63	34.56	35.18	38.91	32.92	75
8	7.5	18.2	−25.0	32.70	34.56	35.49	37.11	33.01	83
9	7.5	16.5	−25.0	32.79	34.47	35.46	36.71	33.04	86
10	8.0	17.7	−25.0	32.79	34.58	35.50	36.94	33.06	90
11	7.7	17.0	−31.3	32.97	34.43	35.21	37.79	33.22	89
12	8.7	17.8	−31.3	33.02	34.63	35.57	37.34	33.27	98
13	8.2	17.7	−31.3	33.02	34.56	35.66	37.74	33.26	96
14	7.5	41.3	−21.5	33.20	38.35	40.67	43.99	34.13	150
15	4.0	17.6	−18.0	33.51	35.70	35.74	42.15	33.87	63

No. 1~5, laboratory data, 6~15, field data. * wind blowing.

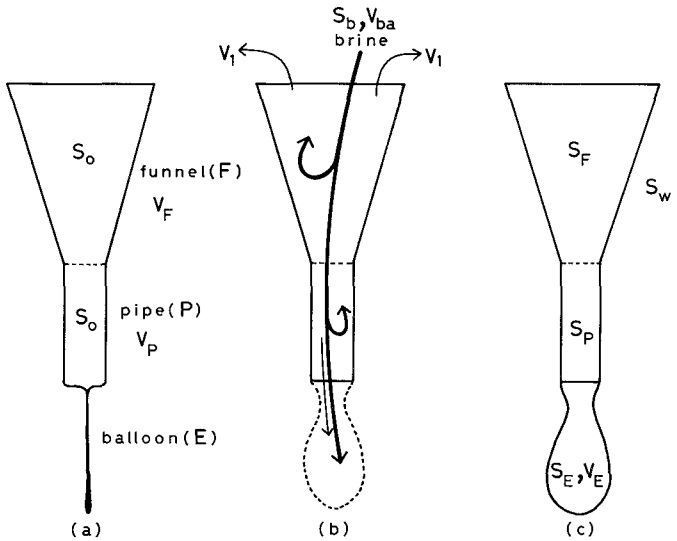

Fig. 25 Modeling on the possible transfers of brine (heavy arrowed lines) and seawater (thin arrowed lines) which may occur in the sampler during the brine collection when (a) $t=0$, (b) $0<t<T$ and (c) $t=T$.
Details in the text.

$$V_j = \int_0^T v_j(t)\,dt \qquad (j = \mathrm{ba},\ 1) \tag{9}$$

where $v_j(t)$ represents the volume of the brine or the seawater at time t during the freezing period in case of j (=ba, 1). Therefore, the mean salinities of them are given by the following :

$$\left.\begin{aligned} \frac{\int_0^T \rho_j(t)\, s_j(t)\, v_j(t)\,dt}{\int_0^T \rho_j(t)\, v_j(t)\,dt} &= S_b\,(j=\mathrm{ba}) \\ \frac{\int_0^T \rho_j(t)\, s_j(t)\, v_j(t)\,dt}{\int_0^T \rho_j(t)\, v_j(t)\,dt} &= S_1\,(j=1) \end{aligned}\right\} \tag{10}$$

where $\rho_j(t)$ and $s_j(t)$ represent, respectively, the density and salinity of the brine or the seawater which are related with the volume $v_j(t)$. According to the basic model proposed in Section V. 1., the only unknown value for determining S_b is S_1. As seen in the model shown in Figure 25, a seawater with salinity S_1 originates from the funnel. Therefore, since a value between the minimum S_o and the maximum S_F should be acceptable for S_1, the following approximation is used to derive S_b :

$$S_1 = (S_o + S_F)/2 = S_{oF}. \tag{11}$$

Introducing the above definitions and approximation in Equations (2) and (3) , we obtain.

$$\rho_b V_{ba} = (\triangle M_s - S_{oF} \triangle M)/((S_b - S_{oF}) \tag{12}$$

where

$$\triangle M = (\rho_F - \rho_o)\ V_F + (\rho_p - \rho_o)\ V_p + \rho_E V_E$$

and

$$\triangle M_s = (\rho_F S_F - \rho_o S_o)\ V_F + (\rho_p S_p - \rho_o S_o)\ V_p + \rho_E S_E V_E \cdot$$

In the above equation, all the amounts except for S_b, ρ_b and V_{ba} are measurable values. The densities of seawater samples were determined, from Knudsen's Hydrographic Table, using measured salinities and the corresponding freezing temperatures [Fujino et al., 1974].

According to the basic model, S_b can be determined by measuring the salinity and the mass of formed sea ice. In case of the conventional method of ice sampling, however, not a little measurement errors are inherent in the measured values of the salinity and the mass because of the unavoidable drainage during the removal of the ice sample from the ice sheet. Therefore, the determination of S_b in the present experiment is made by using the following method. In the laboratory, a closed environment was provided in the tank. Let us represent the surface area of an ice sheet in the tank as A, where $(A-a)$ should be larger than a. Since the amounts of mass and salt are conserved in the tank for $0<t<T$ regardless of the

sublimation of sea ice during the growth process, we obtain

$$\rho_o V_o=\rho_i AI+\rho_w V_w+\rho_R V_R+\rho_F V_F+\rho_P V_P+\rho_E V_E \tag{13}$$

$$\rho_o S_o V_o=\rho_i S_i AI+\rho_w S_w V_w+\rho_R S_R V_R + \rho_F S_F V_F+\rho_P S_P V_P+\rho_E S_E V_E \tag{14}$$

where V_o, V_w and V_R represent the volumes of the original seawater at $t=0$, the remaining seawater at $t=T$ in the tank, and the seawater which flowed out through the pressure relief tube, respectively, and I represents the sea ice thickness ; and S_w, S_R and S_i represent the salinities of the remaining seawater, the seawater which flowed out and the sea ice, respectively. Meanwhile, if the sampler is not placed in the tank, the conservation relations of the amounts of mass and salt become

$$\rho_o V_o=\rho_i AI+\rho_b V_{bA}+\rho_o V_x \tag{15}$$

and

$$\rho_o S_o V_o=\rho_i S_i AI+\rho_b S_b V_{bA}+\rho_o S_o V_x, \tag{16}$$

respectively, where V_{bA} and V_x represent the total volume of brine streamers excluded from the ice area A for $0<t<T$ and the volume of the original seawater not involved in the freezing process, respectively. Using Equations (13) through (16), we have

$$\rho_b V_{bA}=L/(S_b-S_o) \tag{17}$$

where

$$L=(S_w-S_o)\rho_w V_w+(S_R-S_o)\rho_R V_R+(S_F-S_o)\rho_F V_F +(S_P-S_o)\rho_P V_P+(S_E-S_o)\rho_E V_E.$$

In Equation (17), all the amounts except for S_b, ρ_b and V_{bA} are the measurable values.

Next, on the assumption that the streams of brine from the ice front are distributed homogeneously in space, we have

$$\rho_b V_{bA}=\alpha\rho_b V_{ba} \tag{18}$$

where $\alpha=A/a$ (about 8.5~8.8 in the present experiment). The brine collected by the funnel in this experiment consists of two components : one originated from the ice-water interface, as shown in Figure 18, and the other originated from the interior of the ice sheet through brine drainage channels, although the amount of the latter is evidently much smaller than the former. The maximum ice area containing a single brine streamer has been observed to be about 100 cm^2, as shown in Table 1. As mentioned in Section III. 1., the spatial frequency of brine channels has been examined by many investigators. The maximum ice area which contains one brine channel was about 180 cm^2 in a natural thick ice. Meanwhile, in a thin ice that formed in the laboratory, the maximum ice area was about 50 cm^2 at the lowest-

growth rate as shown in Figure 13, A horizontal section of an ice produced at the lowest growth rate in the present experiment is shown in Figure 26. Even at the lowest rate, there exist several brine channels within the ice area covered with the funnel (about 20 cm^2). Therefore, it can be concluded that the funnel size used in the present study is large enough ; thus, the assumption in Equation (18) is acceptable.

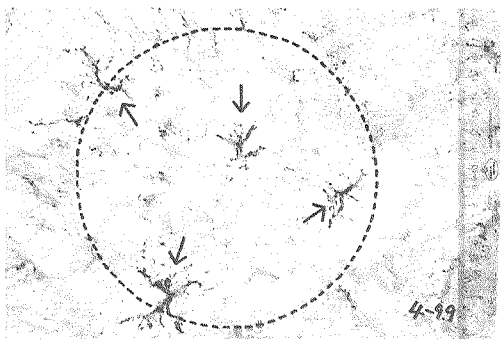

Fig. 26 Horizontal section of sea ice formed at the lowest growth rate. A circle indicates the area covered by the funnel, Several brine channels (indicated by arrows) are visible within this area.

Using this validated assumption, the salinity of the brine excluded in the laboratory experiment is eventually derived from Equations (12), (17) and (18) as

$$S_b = S_o + L(S_{oF} - S_o)/(L - \alpha N) \qquad (19)$$

where $N = \triangle M_S - S_{oF} \triangle M$. In the above equation, it is obvious that S_b depends on the overflow salinity S_{oF}, which is the approximated value. In order to check the justification of the approximation shown in Equation (11), we examined the effect of the variations in S_i on S_b. An example of them is shown in Figure 27 (run 1). The influence on S_b of a $\pm 10\%$ error in $(S_F - S_o)$ for the approximation in Equation (11) was estimated to be less than $\pm 10\%$ at the most. Meanwhile, to check the accuracies of the measured values of the others except for S_{oF} in Equation (19), the sea ice salinity estimated by introducing the values into

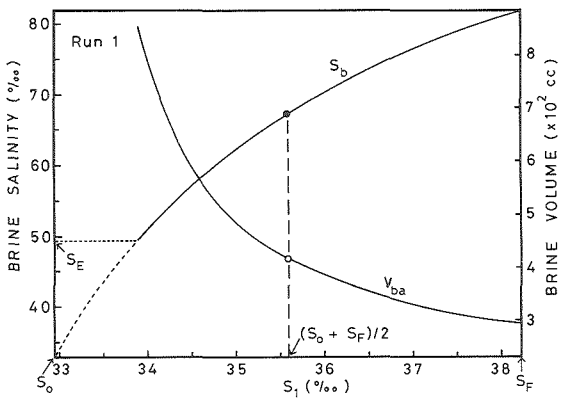

Fig. 27 Effect of change in S_i on S_b and V_{ba} (run 1).

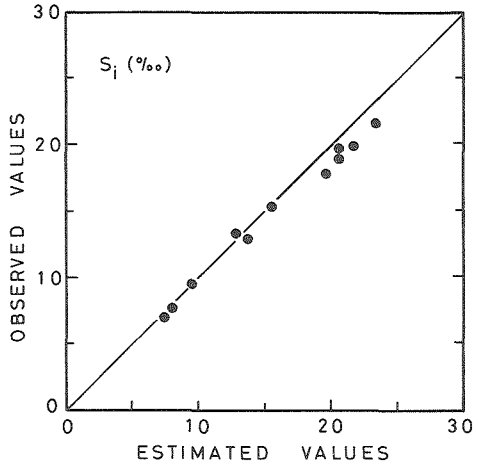

Fig. 28 Comparison between estimated and observed values of sea ice salinity.

Equations (13) and (14) was compared with that actually observed. Then, they were found fairly close to the values represented in Figure 28.

In the field work, however, it is impossible to experimentally examine whether the amounts of mass and salt are conserved in the pool, because it is difficult to measure the exact pool area ; and this causes uncertainty in values of V_w, which represents the seawater volume remaining in the pool after the brine collection is finished. In spite of such circumstances, S_b in the pool experiment can also be determined by introducing the principle of the basic model. Since the capacity of the pool is about 30 times larger than of the tank, the effect on S_w of the seawater (V_1) which overflowed from the brine sampler is negligible. Since the sea ice which formed in the large experimental pool, unlike that in the small tank, seemed to be isostatic, it is unnecessary to consider the water overflow due to the ice growth.

With all the above considerations, we obtain

$$\rho_b V_{ba}=(S_w-S_o)\rho_w a h_w/(S_b-S_o) \tag{20}$$

where h_w represents a depth of the water column, or a mean length from the bottom of sea ice to the floor of the pool. From Equations (12) and (20), the brine salinity in the pool experiment becomes

$$S_b=S_o+W(S_{oF}-S_o)/(W-N) \tag{21}$$

where $W=(S_w-S_o)\rho_w a h_w$. Thus S_b can be obtained from the measured values by introducing the approximation in Equation (11) used for the laboratory experiment.

Using the values of S_b thus determined, the mass of brine streamers can be derived from Equations (12) or (20). The density of brine within sea ice, the concentration of which attaining to the thermodynamical equilibrium, is approximately expressed as $\rho_b=1+0.008S_b$ [e. g. Ono, 1968]. Therefore, the volume V_{ba} of brine can also be determined from Equations (12) or (20), by using the above approximation. The influence of the error in S_1 on V_{ba} is shown in Figure 27 as an example (run 1).

V. 4. *Effect of ice growth rate*

The values of S_b and V_{ba} determined under different experimental conditions are shown in Table 3.

Shown in Figure 29 is the salinity ratio of brine to original seawater, S_b/S_o, as a function of ice growth rate. The brine salinity increases remarkably as the ice growth rate decreases. The maximum brine salinity is higher than S_o by about 2.7 time ; it corresponds to about 93‰ when the salinity of the original seawater is 33.0‰. Even at the highest ice growth rate, S_b exceeds S_o by about 1.3 times.

Meanwhile, the volume flux of the brine decreases with decreasing ice growth rate, as shown in Figure 30. Added to this figure are the previous data which were obtained by analyzing schlieren movie films. They yield similar results to the present data. It is clear

Table 3 Summary of Analytical Results

Experiment Number (No)	Brine Salinity (‰)	Brine Volume (cc)	Salt Flux ($g \cdot cm^{-2} \cdot s^{-1}$)	Volume Flux ($cc \cdot cm^{-2} \cdot s^{-1}$)	V_E / V_{ba}
1	67.14	417	8.04×10^{-7}	1.14×10^{-5}	0.38
2	62.58	409	9.46	1.44	0.35
3－I	73.09	418	7.06	0.91	0.41
3－II	78.67	331	7.63	0.91	0.42
3－III	84.49	317	7.07	0.78	0.38
4－I	87.58	370	6.92	0.74	0.51
4－II	94.27	337	6.36	0.63	0.46
4－III	96.00	291	6.69	0.65	0.44
5－I	58.84	337	11.54	1.87	0.33
5－II	65.22	305	12.25	1.78	0.31
5－III	71.64	328	9.28	1.22	0.37
6	51.41	285	11.61	2.17	0.24
7	46.77	338	12.80	2.64	0.22
8	43.66	419	14.49	3.20	0.20
9	43.80	376	14.35	3.17	0.23
10	43.93	396	14.17	3.11	0.23
11	42.28	403	14.39	3.29	0.22
12	42.51	430	14.74	3.35	0.23
13	42.27	424	14.59	3.33	0.23
14	62.69	466	10.34	1.57	0.32
15	54.99	246	11.15	1.94	0.26

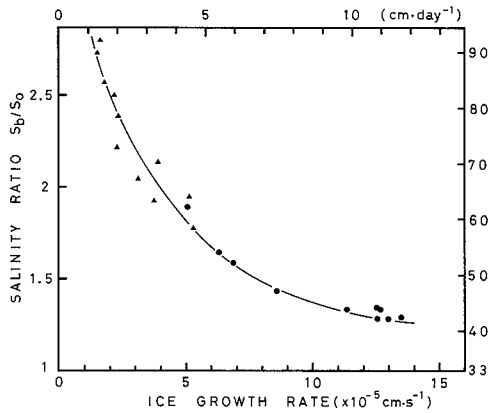

Fig. 29 Brine salinity vs. ice growth rate. Left ordinate, salinity ratio of brine to original seawater (S_b/S_o) ; right ordinate, brine salinity for original seawater salinity of 33.0‰ .

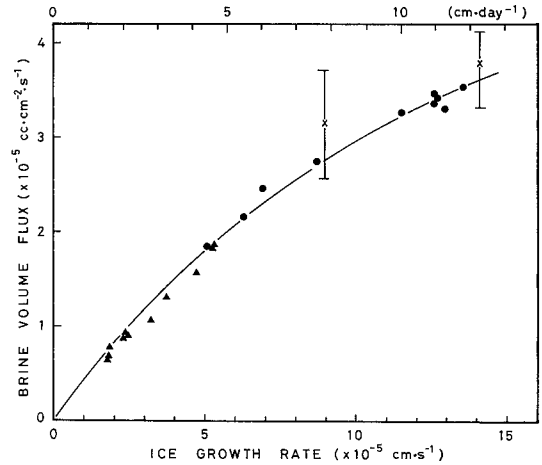

Fig. 30 Volume flux of brine vs. ice growth rate. Circle, field data ; triangle, laboratory data ; cross, data obtained by analyzing schlieren movie films (bar indicates a limited analysis of the movie films).

from Figures 29 and 30 that a smaller amount of brine with a higher salinity is excluded from growing sea ice at a lower growth rate. The above quantitative results support the characteristics of the excluded brine which were obtained previously with a schlieren optical system (see Figure 18); at a lower growth rate a smaller number of thicker brine fell into the seawater. Although a distinct cause of such a brine exclusion process is unknown as yet, the following explanation satisfies us qualitatively. At a lower growth rate, a larger size of ice platelets forms slowly at a growing ice front. Therefore, during the slower formation of the ice platelets, the concentrated, saline brine is excluded at a slower speed.

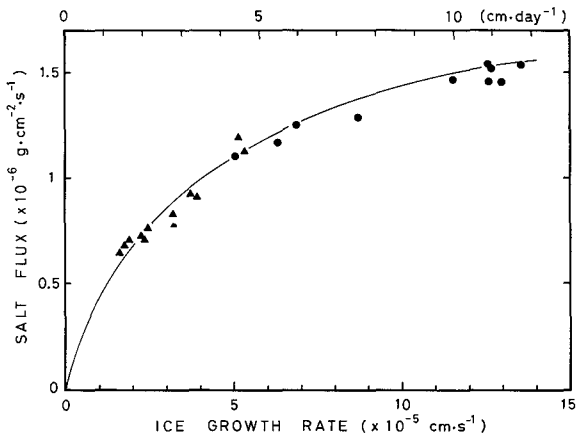

Fig. 31 Salt flux of brine vs. ice growth rate. Circle, field data ; triangle, laboratory data.

The flux of salt shown in Figure 31, which was estimated using S_b and the brine volume flux, decreases as the ice growth rate decreases. Figures 29, 30 and 31 demonstrate that all the salinity, the volume flux and the salt flux of brine depend upon the ice growth rate and also that the salt flux depends largely upon the volume flux rather than the brine salinity. The good dependencies of those upon the ice growth rate imply that the brine sampler used and the method for determining S_b are reasonable.

V. 5. *Effect of increase in ice thickness*

The effect of an increase in ice thickness on S_b and V_{ba} is shown in Figure 32a. The effect was examined, in the laboratory experiment, at three constant ice growth rates, A, B, and C ($A>B>C$), as also seen in Figure 24. At any constant growth rate, S_b increases but V_{ba} decreases with an increase in ice thickness (from stage I to stage III). The absolute values of S_b and V_{ba} in each stage increase with a decrease in ice growth rate, as shown in Figure 32a. In spite of marked changes in both values with the ice thickness, the salt-mass of brine ($\rho_b S_b V_{ba}$) changes little, as shown in Figure 32b. However, $\rho_b S_b V_{ba}$ increases at any stage with a decrease in ice growth rate.

The rate of ice growth decreases generally with an increase in ice thickness. To examine how the salinity, the volume flux and the salt flux of brine change with such ice growth, a hypothetical process of ice growth was introduced, as shown in Figure 33a. This process is composed of three constant growth rates ; namely, ice grows at the highest, the intermediate and the lowest rate, respectively, at stages I, II and III. Although the combination of three ices with different growth rates is of course unreal, this process of ice

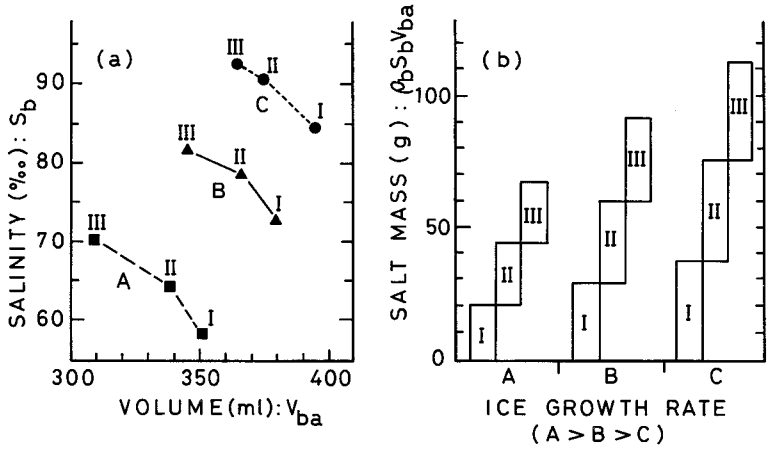

Fig. 32 Effect of an increase in ice thickness on S_b, V_{ba} and $\rho_b S_b V_{ba}$. (a) S_b vs. V_{ba} ; (b) $\rho_b S_b V_{ba}$ vs. ice growth rate. A, B and C correspond to three constant growth rates given in Fig. 24. Stages I , II and III correspond to the periods of brine collection shown in Fig. 24. The amounts of $\rho_b S_b V_{ba}$ are represented by the heights of rectangles.

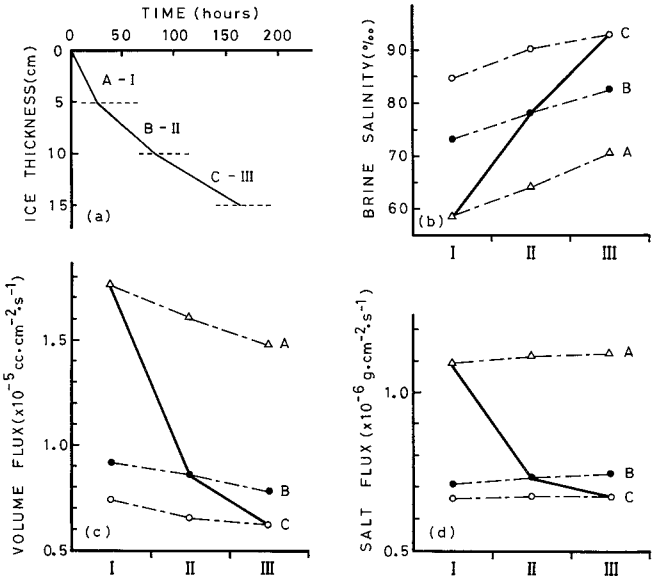

Fig. 33 Changes in (b) salinity, (c) volume flux and (d) salt flux of brine with (a) a hypothetical process of ice growth. Various marks correspond to those indicated in Figs. 24 or 32. Details in the text.

growth constitutes a general character from the view point of the ice growth rate. Because of the combined effect of the ice growth rate and the ice-thickness increase, both the tendencies of an increase in brine salinity and a decrease in brine volume flux with an increase in ice thickness are further accelerated in such an ice growing process, as shown in Figures 33b and 33c. The resultant salt flux also decreases with an increase in ice thickness, depending upon the volume flux. As shown in Figure 33d, a marked decrease in salt flux is due only to the effect of the ice growth rate since the salt flux is affected little by the increasing of ice thickness at a constant growth rate.

It is suggested from Figure 33 that all the salinity, the volume flux and the salt flux of brine excluded depend largely upon the ice growth rate changing momentarily during the ice growing process, and hence that the contribution of brine exclusion to the polar ocean is predominant in the growth process of a thin ice with a higher growth rate rather than that of a thick ice.

V. 6. *Brine exclusion process*

We have clarified quantitatively the effect of both the ice growth rate and the ice-thickness increase on the exclusion of brine. In addition, we have also pointed out that a greater contribution of brine exclusion to the polar ocean is made by the growth of thinner sea ice. Differential expressions such as ice growth rate, volume flux and salt flux have been used in arguing the foregoing. To understand the brine exclusion process from a practical point of view, however, it will be better to use integral expressions since values easily obtainable by measurements in the field are such integrated values as ice thickness and time required for ice formation.

Shown in Figure 34a are the salinity and the volume of brine which was excluded during the formation of ice in relation to the ice thickness and its formation time. It was produced on the basis of the raw data obtained in the present experiment. In the figure isosalinities and isovolumes are represented by solid and dot-dash lines, respectively. In order to understand the significance of this figure exactly, let us explain it by using one example marked with ⊙. This example implies that about three days were required for the formation of sea ice about 5 cm in thickness and that brine about 2 cc in volume, with a salinity of about 80‰ , was excluded through unit ice area during the time of formation. Hence, when a knowledge is sought in field work in future about the salinity and volume of the excluded brine, it will be satisfied by this figure and measurements of only ice thickness and its formation time.

Another piece of significant information is also contained in Figure 34a, as follows : Now let us imagine any straight line which passes the origin of the coordinate axes in the figure. Then, it will be readily recognized that the gradient of the straight line corresponds to the ice growth rate. Therefore it can also be understood from this figure that the brine salinity depends primarily upon the ice growth rate ; namely, its salinity increases with decreasing ice

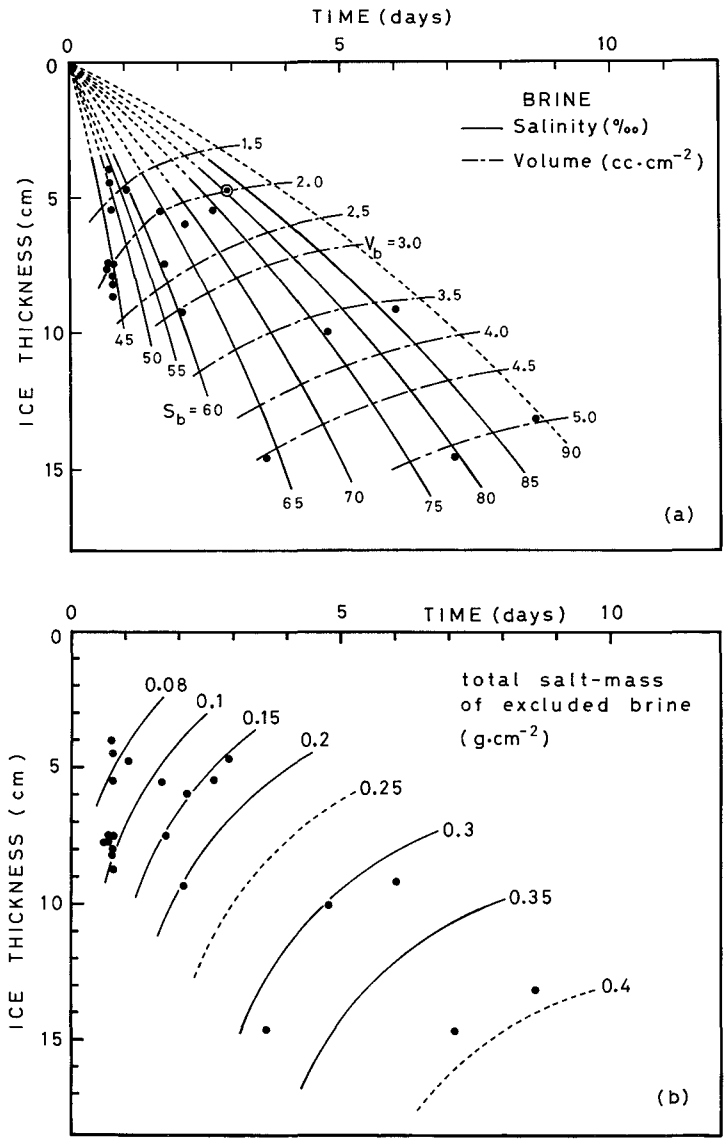

Fig. 34 Changes in (a) salinity and volume and (b) salt mass of brine excluded with the formation time required and the thickness of original sea ice. Solid and dot-dash lines indicate, respectively, isosalinities and isovolumes (a) drawn on the basis of measured values (dots). An explanation is given in the text concerning the mark (⊙), which represents one of the measured values.

growth rate. Meanwhile, the brine volume depends upon the time required for ice formation as well as the ice growth rate ; its volume increases with increasing growth rate and formation time. The increase in brine volume is therefore accelerated as the amount of ice grown increases. Because of the strong volume dependence of the salt-mass of brine, the salt-mass also increases with increasing amount of ice grown, as shown in Figure 34b.

The salinity and volume of the excluded brine have been derived by collecting it actually. Whether these results are acceptable or not can be confirmed at present only by means of sea ice salinity ; downward salt flux through the ice-water interface can be estimated not only from the brine salinity and volume, but also from the sea ice salinity, as mentioned in Section III.

A comparison was made between the values of salt flux which were estimated using the above two different kinds of methods. These results are represented in Figure 35, which are composed of Figure 16 (estimated from the sea ice salinity) and Figure 31 (given by means of the brine salinity and volume). A fairly good agreement between both the estimated values as a function of ice growth rate demonstrates that our results concerning the brine salinity and volume should be applicable under other various natural conditions. An effort will be made accordingly to explain the change in sea ice salinity with ice growing conditions, using our data on brine exclusion. These explanations will be made referring to the two figures, Figures 14 and 34, which were already proposed. The salinity of a sea ice with any given

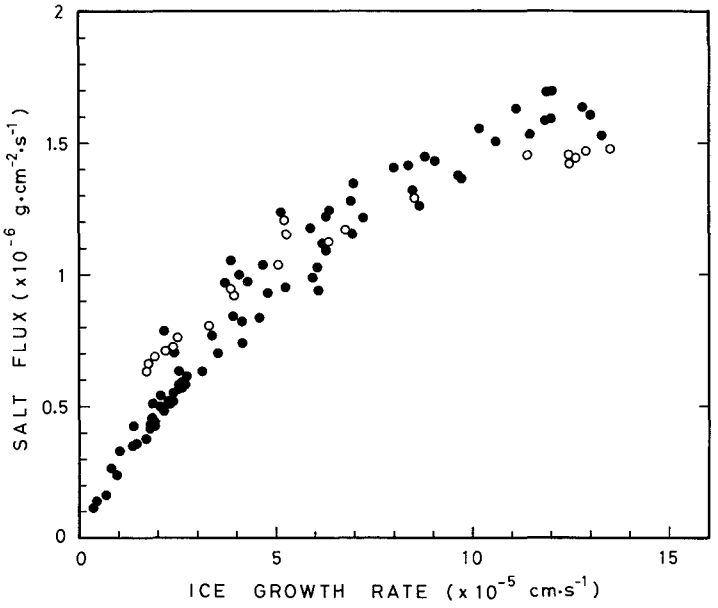

Fig. 35 Comparisons of salt flux between values (○) obtained by brine collection and values (●) estimated from sea ice salinity.

thickness decreases as its formation time increases, as shown in Figure 14. The decrease in sea ice salinity with time is caused as the result of the following brine exclusion process : a larger amount of brine with a higher salinity is excluded from a sea ice which requires a relatively long time to grow to the fixed thickness, resulting in the exclusion of a larger amount of salt, as is clearly understood from Figure 34.

Meanwhile, a sea ice which forms during any fixed time has a higher salinity as it is thicker, as shown in Figure 14. Viewing this situation from a standpoint of brine exclusion, a larger amount of brine with a lower salinity is excluded from a relatively thick sea ice, resulting in the exclusion of a larger amount of salt, as shown in Figure 34. It is concluded from the above results that a thicker sea ice which forms during a fixed time has a higher salinity in spite of the exclusion of brine with a larger amount of salt from the sea ice. Although this conclusion is apparently curious, its validity will be verified by recollecting the definition of a sea ice salinity here.

The salinity of a sea ice tested represents the mean value throughout an entire sea ice column and is defined as the mass ratio of the contained brine-salt to the entire column. If the contained brine is assumed to distribute homogeneously in space, therefore, the sea ice salinity should be determined by the salt mass of brine which is contained per any *unit mass* of sea ice in the column.

Meanwhile, the mass of salt excluded as brine from the sea ice column represents the *integrated, total amount* throughout the period during the formation of the sea ice column.

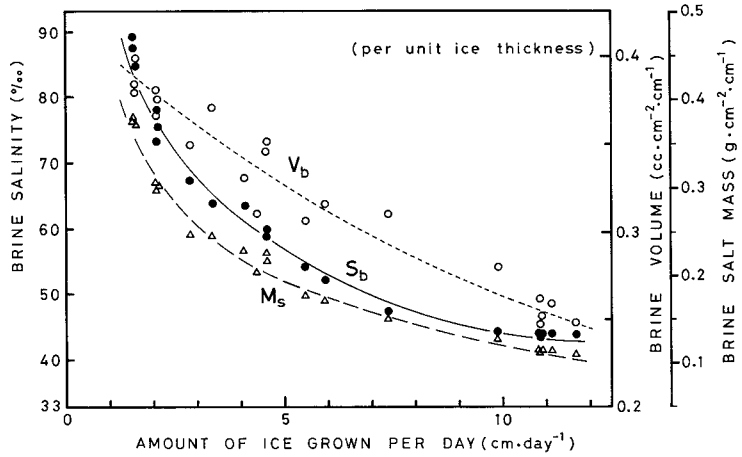

Fig. 36 Brine exclusion process. Abscissa, amount of ice grown per day ; ordinate, salinity (●), volume (○) and salt mass (△) of brine which was excluded per unit amount of ice grown.

We therefore need to use the mass of salt excluded per unit mass of sea ice grown, in interpreting the change in sea ice salinity with thickness in terms of brine exclusion. The apparently curious conclusion proposed above is caused by the use of the total mass of excluded salt. As shown in Figure 36, the exclusion of a smaller amount of brine with a lower salinity per unit mass of ice grown comes about from a sea ice which grows thickly during the fixed time (one day) ; consequently a smaller mass of salt is excluded, resulting in a higher salinity of the thicker sea ice.

VI. Concluding remarks

The exclusion process of brine from growing sea ice, which plays an important role in the polar ocean, has been quantitatively treated in this study. The results obtained are summarized as follows :

(1) Oceanographic observations during the Antarctic winter disclosed the salinization of shelf water and a change in water salinity structure from stratified to homogenized distribution with progress in sea ice growth. These phenomena, which were observed in the seawater under the fast ice sheet near Syowa Station (by making a pool) and under the fast ice cover near the Sôya Coast (by boring holes), came about as a result of the haline convection induced by brine exclusion during the growth of ice. The thickness of convection layers changed with the amount of ice grown ; namely, under the pool the convection layer reached to a depth of 40 m at its maximum when the thickness of sea ice grew to about 0.25 m, whereas it reached to a depth of 400 m at its maximum under the fast ice cover during the time in which the thickness of the fast ice grew to a range from about 0.8 to 2 m. The foregoing observations suggest that the brine exclusion process has the primary influence upon the oceanic phenomena in the polar region.

(2) The falling of brine into seawater was experimentally observed with a schlieren optical system. The brine was excluded from fixed positions at the ice-water interface. While falling down into the seawater, the excluded brine formed long vertical filaments without appreciable diffusion. These observations disclosed that the diameter and falling velocity of the brine filaments and their number vary with the growth rate of sea ice ; for instance, at a higher rate a larger number of finer brine filaments fell at a lower velocity.

(3) Direct measurements were made of the salinity and volume of excluded brine under various ice growing conditions. All of the salinity, volume flux and salt flux of the brine depended upon the ice growth rate. The brine salinity increased with decreasing ice growth rate and the maximum salinity was about 93‰ for an original seawater salinity of 33.0‰ . Both the volume flux and salt flux increased with increasing ice growth rate ; hence, the salt-mass of brine excluded depended highly upon its volume rather than its salinity. Therefore, the major contribution of brine exclusion to the ocean is made by a thinner sea ice which grows at a higher rate since the growth rate of a natural sea ice generally decreases with

increasing thickness.

(4) The brine volume, which is an integrated quantity, depends upon the time required for ice formation as well as the ice growth rate ; namely, the volume increases with an increase in both. Accordingly it is suggested that the brine volume increases with an increase in amount of ice grown.

(5) A change in sea ice salinity under various ice growing conditions can be understood from the following result of observations of the brine exclusion process : A lower salinity in a sea ice that consumes a longer time to grow to a fixed thickness is due to the exclusion of a larger amount of brine with a higher salinity during its growth. Meanwhile, a higher salinity in a thicker sea ice that forms during a fixed time is due to the exclusion of a smaller amount of brine with a lower salinity per unit mass of ice grown during the period. These results suggest that in future the salinity and volume of brine excluded during the formation of a sea ice can be estimated approximately by measuring the formation time, thickness and salinity of the sea ice.

All the above results also provide the following significant suggestion : A greater contribution of brine exclusion to the ocean is made by a higher ice production during such a limited period of the year as winter ; a marginal ice zone, where ice sheets coexist with open waters, corresponds to the area of high ice production in the polar ocean. This suggestion is based on the result of the present study ; that is, the amount of salt which is excluded as brine from sea ice into seawater depends greatly upon the volume of the brine rather than the salinity of it ; and this volume increases with increasing amount of ice grown. In connection with this suggestion, this study points to the importance of further oceanographic observations in the marginal ice zone in winter.

Acknowledgements

The author would like to express his deep thanks to Professor N. Ono and the late Professor T. Tabata of Hokkaido University for their suggestions and encouragement throughout this study, and to Professors Y. Suzuki, S. Kanari and M. Aota of the same university for their useful comments and critical reading of the original paper. He also wishes to express his heartful gratitude to Professor S. Martin of University of Washington and Professor K. Kusunoki of the National Institute of Polar Research for their valuable suggestions and critical reading of part of this paper. He is also grateful to Professor T. Yoshino of University of Electro-Communications and all the members of the wintering party of the 17th Japanese Antarctic Research Expedition for their kind support on the field work in Antarctica, and to Dr. J. F. Kelley and the staffs of Naval Arctic Research Laboratory for their help and support on the field work at Barrow, Alaska. His thanks are also due to Messrs. T. Kawamura, T. Takizawa and T. Saito for their kind discussion and help in this study.

References

Bennington, K. O. 1963 Some crystal growth features of sea ice. *J. Glaciol.*, **4**, 669-688.
Bennington, K. O. 1967 Desalination features in natural sea ice. *J. Glaciol.*, **6**, 845-857.
Brennecke, W. 1921 Die ozeanographischen arbeiten der deutschen antarktischen expedition 1911-1912. *Archiv der Deutschen Seewarte*, **39** (1), 214p.
Cox, G. F. N. and Weeks, W. F. 1975 Brine drainage and initial salt entrapment in sodium chloride ice. *CRREL Research Report*, **345.**
Farhadieh, R. and Tankin, R. S. 1972 Interferometric study of freezing of sea water. *J. Geophys. Res.*, **77**, 1647-1657.
Foster, T. D. 1969 Experiments on haline convection induced by the freezing of sea water. *J. Geophys. Res.*, **74**, 6967-6974.
Foster, T. D. 1972 Haline convection in polynyas and leads. *J. Phys. Oceanogr.*, **2**, 462-469.
Fujino, K., Lewis, E. L. and Perkin, R. G. 1974 The freezing point of seawater at pressures up to 100 bars. *J. Geophys. Res.*, **79**, 1792-1797.
Fujiwara, K. 1971 Soundings and submarine topography of the glaciated continental shelf in Lützow-Holm Bay, East Antarctica. *Antarctic Rec.*, **41**, 81-103.
Gill, A. E. 1973 Circulation and bottom water production in the weddell Sea. *Deep-Sea Res.*, **20**, 111-140.
Lake, R. A. and Lewis, E. L. 1970 Salt rejection by sea ice during growth. *J. Geophys. Rec.*, **75**, 583-597.
Martin, S. 1979 A field study of brine drainage and oil entrainment in first year sea ice. *J. Glaciol.*, **22**, 473-502.
Mosby, H. 1934 The waters of the Atlantic Antarctic Ocean. *Det. Norske Vieden. Akad., Sci. Res., Norwegian Antarctic Exped.*, 1927-1928, **1** (11), 117p.
Ono, N. 1968 Thermal properties of sea ice. IV. Thermal constants of sea ice. *Low Temp. Sci., Ser.* **A 26**, 329-349.
Saito, T. and Ono, N. 1980 Percolation of sea ice. II. Brine drainage channels in young sea ice. *Low Temp. Sci., Ser.* **A 39**, 127-132.
Tabata, T. and Ono, N. 1957 On the structure of sea ice. *Low Temp. Sci., Ser.* **A 16**, 197-210.
Untersteiner, N. 1968 Natural desalination and equilibrium salinity profile of old sea ice. *J. Geophys. Res.*, **73**, 1251-1257.
Wakatsuchi, M. 1977 Experiments on haline convection occurring under growing sea ice. *Low Temp. Sci., Ser.* **A 35**, 249-258.
Wakatsuchi, M. 1982 Seasonal variations in water structure under fast ice near Syowa Station, Antarctica, in 1976. *Antarctic Rec.*, **74**, 85-108.
Wakatsuchi, M., Takizawa, T. and Saito, T. 1982 On brine drainage channels. *Low Temp. Sci., Ser.* **A 41**, 233-236.
Wakatsuchi, M. and Ono, N. 1983 Measurements of salinity and volume of brine excluded from growing sea ice. *J. Geophys. Res.*, **88**, C5, 2943-2951.
Weeks, W. F. 1958 The structure of sea ice. In Arctic Sea Ice, NAS-NRC Pub. No. 598, 96-99.
Weeks, W. F. and Lee, O. S. 1958 Observations on the physical properties of sea-ice at Hopedale, Labrador. *Arctic*, **11**, 134-155.